doi:10.1093/brain/awp231 Brain 2009: 132; 3122–3133 | 3122

BRAIN
A JOURNAL OF NEUROLOGY

Cutting your nerve changes your brain

Keri S. Taylor,[1,2] Dimitri J. Anastakis[2,3,4] and Karen D. Davis[1,2,3]

1 Division of Brain, Imaging and Behaviour – Systems Neuroscience, Toronto Western Research Institute, University Health Network, Toronto, Canada M5T2S8
2 Institute of Medical Science, University of Toronto, Canada
3 Department of Surgery, University of Toronto, Canada
4 Clinical Studies Resource Centre, Toronto Western Research Institute, University Health Network, Toronto, Canada M5T2S8

Correspondence to: Karen D. Davis, Ph.D.,
Division of Brain, Imaging and Behaviour – Systems Neuroscience,
Toronto Western Research Institute,
Toronto Western Hospital,
University Health Network,
Room MP14-306, 399 Bathurst Street,
Toronto, Ontario,
Canada M5T 2S8
E-mail: kdavis@uhnres.utoronto.ca

Following upper limb peripheral nerve transection and surgical repair, some patients regain good sensorimotor function while others do not. Understanding peripheral and central mechanisms that contribute to recovery may facilitate the development of new therapeutic interventions. Plasticity following peripheral nerve transection has been demonstrated throughout the neuroaxis in animal models of nerve injury. However, the brain changes that occur following peripheral nerve transection and surgical repair in humans have not been examined. Furthermore, the extent to which peripheral nerve regeneration influences functional and structural brain changes has not been characterized. Therefore, we asked whether functional changes are accompanied by grey and/or white matter structural changes and whether these changes relate to sensory recovery? To address these key issues we (i) assessed peripheral nerve regeneration; (ii) measured functional magnetic resonance imaging brain activation (blood oxygen level dependent signal; BOLD) in response to a vibrotactile stimulus; (iii) examined grey and white matter structural brain plasticity; and (iv) correlated sensory recovery measures with grey matter changes in peripheral nerve transection and surgical repair patients. Compared to each patient's healthy contralesional nerve, transected nerves have impaired nerve conduction 1.5 years after transection and repair, conducting with decreased amplitude and increased latency. Compared to healthy controls, peripheral nerve transection and surgical repair patients had altered blood oxygen level dependent signal activity in the contralesional primary and secondary somatosensory cortices, and in a set of brain areas known as the 'task positive network'. In addition, grey matter reductions were identified in several brain areas, including the contralesional primary and secondary somatosensory cortices, in the same areas where blood oxygen level dependent signal reductions were identified. Furthermore, grey matter thinning in the post-central gyrus was negatively correlated with measures of sensory recovery (mechanical and vibration detection) demonstrating a clear link between function and structure. Finally, we identified reduced white matter fractional anisotropy in the right insula in a region that also demonstrated reduced grey matter. These results provide insight into brain plasticity and structure-function-behavioural relationships following nerve injury and have important therapeutic implications.

Keywords: cortical thickness; fMRI; diffusion tensor imaging; plasticity; peripheral nerve injury

Abbreviations: BA = Brodmann area; BOLD = blood oxygen level dependent; fMRI = functional magnetic resonance imaging; PNIr = peripheral nerve transection and surgical repair; S1 = primary somatosensory cortex; S2 = secondary somatosensory cortex

Received April 27, 2009. Revised July 2, 2009. Accepted July 25, 2009. Advance Access publication September 8, 2009

Introduction

Following upper limb peripheral nerve transection and surgical repair (PNIr), ~25% of patients have not returned to work 1.5 years after surgery (Jaquet *et al*., 2001). In addition, ~57% of patients with nerve injuries are between 16–35 years of age (McAllister *et al*., 1996); thus, a long life of disability and economic difficulties may accompany upper limb nerve transection. Understanding the central and peripheral ramifications of peripheral nerve injury may facilitate the development of new therapeutic strategies and intervention programs.

It is not known how the brain responds to PNIr in humans. However, animal studies have established that plasticity within the somatosensory cortex begins immediately following peripheral nerve transection, and that 1 year after complete nerve transection and surgical repair, cortical maps contain patchy, non-continuous representations of the transected and adjacent nerves (Wall *et al*., 1986). The mechanisms that facilitate functional plasticity are thought to include the immediate unmasking of pre-existing projections from adjacent cortical and subcortical levels, and long term sprouting of axons at multiple levels of the neuroaxis, including the primary somatosensory cortex (S1) (Florence and Kaas, 1995; Hickmott and Steen, 2005).

Human brain imaging studies have corroborated the findings from animal models with the identification of altered functional MRI activation maps due to spinal cord injury, amputation, toe-to-thumb transfer, and in patients with carpel tunnel syndrome (Lotze *et al*., 2001; Manduch *et al*., 2002; Jurkiewicz *et al*., 2006; Napadow *et al*., 2006). Furthermore, structural MRI studies have recently visualized grey and white matter changes following traumatic injuries and in diverse pathological conditions, including limb amputation and chronic pain (Apkarian *et al*., 2004; Draganski *et al*., 2006; Davis *et al*., 2008; Geha *et al*., 2008; May, 2008). Grey matter changes are thought to be related to changes in cell size, atrophy and/or loss of neurons or glia, whereas white matter changes are impacted by axonal degeneration and loss of myelin (Beaulieu, 2002; May, 2008).

A powerful approach to delineate mechanisms of pathology and plasticity is to combine functional and structural grey and white matter imaging techniques. We previously reported that patients with complete upper limb PNIr retained profound somatosensory deficits that persist >1.5 years following surgery (Taylor *et al*., 2008*a*). Based on these findings, we reasoned these patients would exhibit functional and structural brain changes in key somatosensory brain areas. Therefore, in this study, we hypothesized that PNIr patients would have: (i) reduced blood oxygen level dependent (BOLD) responses to vibratory stimulation of the transected nerve territory, in the region of S1 that represents the injured upper limb and in the secondary somatosensory cortex (S2); (ii) a corresponding reduction in cortical thickness in these regions of the contralesional S1 and S2; (iii) a correlation between changes in cortical thickness and psychophysical measures of somatosensory function (vibration and touch detection thresholds); and (iv) reduced fractional anisotropy (a measure of white matter integrity) in white matter feeding into/out of these somatosensory cortical areas.

Methods

Subjects

We recruited 27 patients with complete transection of the median and/or ulnar nerve followed by surgical repair from plastic surgeons affiliated with the University of Toronto Hand Program between June 2006 and May 2008. From this larger cohort, 14 pain-free patients (three females, 11 males; 34 ± 10 years) with complete transection of the right median and/or ulnar nerve were included in the study [to avoid confounds related to the presence of pain and laterality patients with pain ($n = 6$) and left sided lesions ($n = 7$) were excluded from this analysis]. All patients underwent microsurgical nerve repair at least 1.5 years prior to study enrolment (recovery time varied from 1.5 to 8 years). In addition, we recruited 14 age- and sex-matched healthy controls (3 females, 11 males; 34 ± 10 years). All subjects gave informed written consent to procedures approved by the University Health Network Research Ethics Board. All subjects were right handed (determined using the Edinburgh handedness inventory: Oldfield, 1971) and had no history of neurological injury or chronic pain (either before or after nerve transection). See Table 1 for demographic details.

Study design

All subjects participated in an imaging session that included: (i) functional magnetic resonance imaging (fMRI) in response to vibrotactile stimuli applied to the right index finger (within the median nerve territory); (ii) a high-resolution anatomical scan of the whole brain, acquired for image registration and for the analysis of cortical grey matter; and (iii) two diffusion tensor imaging scans for the assessment of white matter integrity. Prior to imaging, subjects were instructed in the basic design of the experiment and reminded to remain as still as possible throughout the duration of the scan. Subjects were free to

Table 1 Demographic details

	PNIr ($n = 14$)	HC ($n = 14$)
Sex		
No. of males	11	11
No. of females	3	3
Age at assessment (years)	34 ± 10	34 ± 10
Average time from surgery (years)	4.8 ± 3	–
Handedness	Right	Right
Hand affected	Right	–
Nerve transected (#)		
Median	9	–
Ulnar	3	–
Median and ulnar	2	–
No. of subjects in each analysis		
Nerve conduction	9	–
fMRI	11	11
CTA $_{group\ comp}$	14	14
CTA $_{correlation}$	13	–
DTI	14	14

HC = healthy controls, PNIr = peripheral nerve injury and surgical repair patients, fMRI = functional magnetic resonance imaging, CTA $_{group\ comp}$ = cortical thickness analysis group comparison, CTA $_{correlation}$ = cortical thickness analysis correlation analysis, DTI = diffusion tensor imaging.
Times are means ± SD

withdraw from the study at any time. In addition, a sensory and motor assessment was performed for all subjects (Taylor *et al*., 2008*a*). As touch and vibration detection thresholds were correlated with cortical thickness a description of these methods is included below (other psychophysical measures will be reported elsewhere).

Vibration threshold

Vibration detection thresholds were determined using a hand held Bio-Thesiometer (Bio-Medical Instrument Company, USA). The device has a 12-mm probe that was placed on the distal phalanx of the right index finger (D2). Thresholds were determined using the method of limits: the amplitude (voltage) was gradually increased until the subject indicated that they perceived the stimulus. Vibration thresholds were acquired three times and an average value was calculated. During vibration threshold testing, subjects were instructed to close their eyes and rest the back of their hand on a supportive cushion.

Mechanical detection threshold

Mechanical detection thresholds were determined using a standardized set of von Frey filaments (OptiHair$_2$ Marstock Nervtest, Germany) containing 12 logarithmically spaced calibrated filaments that delivered forces from 0.25–512 mN. The contact surface diameter of all 12 filaments was ~0.4 mm. Trials were conducted with the subject's eyes closed and hands resting on a soft cushion. Probes were applied in an ascending series and subjects were required to make a response every time they felt a probe touch the right D2 fingertip. This process was repeated three times. The force for the filament that was detected in at least two of three trials was reported as that subject's mechanical detection threshold.

Nerve conduction testing

Patients participated in bilateral sensory and motor nerve conduction studies at the Toronto Western Hospital electromyography (EMG) clinic. For motor nerve conduction, the stimulating electrode was placed at the wrist and elbow (separately) and the recording electrode was placed over the abductor pollicis brevis, for median nerve assessment, or the abductor digiti minimi for ulnar nerve assessment. For sensory nerve testing the recording electrode was placed at the wrist and the stimulating electrode was placed at digits D2, D3 and D5. A senior, experienced neurologist from the Toronto Western Hospital EMG Clinic (Dr Peter Ashby) reviewed all clinical assessments to determine which nerves demonstrated normal/abnormal responses. As amplitude and latency measures are known to vary substantially between subjects (due to factors such as the density of innervation, the depth of the nerve and the thickness of an individual subject's skin) (Kimura, 2001) each patient's untransected nerve served as their own control for comparison with values from the transected side. In those patients with detectable nerve conduction responses, paired *t*-tests were performed to assess the difference in latency or amplitude measures between each patient's transected and contralesional untransected nerves.

Imaging parameters

Brain imaging data were acquired using a 3T GE MRI system fitted with an eight-channel phased array head coil. Subjects were placed supine on the MRI table and each subjects' head was padded to reduce movement. Whole-brain fMRI data was acquired using echo planar imaging (28 axial slices, field of view (FOV) = 20 × 20 cm, 64 × 64 matrix, 3.125 × 3.125 × 4 mm voxels, echo time (TE) = 30 ms, repetition time (TR) = 2000 ms). The scan time was 5 min and 8 s (154 frames). During scanning, a non-painful, 12 Hz vibrotactile stimulus was applied to the distal phalanx of the right D2 using balloon diaphragms driven by compressed air (Device manufactured by Dr Christo Pantev; www.biomag.uni-muenster.de). Stimuli were delivered in blocks of 10 s interleaved with 20 s of rest, for a total of 10 blocks of stimulation and 10 blocks of rest. The first 8 s (4 TRs) of data acquired from each run were discarded to allow for fMRI signal equilibration. Subjects were instructed to keep their eyes closed throughout scanning and focus on the stimuli. A whole brain three dimensional (3D) high-resolution anatomical scan (124 sagittal slices, 24 × 24 cm FOV, 256 × 256 matrix, 1.5 × 0.94 × 0.94 mm voxels) was acquired with a T_1-weighted 3D spoiled gradient echo sequence (one signal average, flip angle = 20°, TE ~5 ms). In addition, two diffusion tensor imaging scans (38 axial slices, FOV 24 × 24 cm, 128 × 128 matrix, 1.875 × 1.875 × 3 mm voxels) were acquired along 23 directions with a *b*-value of 1000 s mm^{-2}. Each run also contained two volumes with no diffusion weighting.

fMRI analysis

Data were analysed using Brainvoyager QX v1.8 (Brain Innovaton, Maastricht, Netherlands). Pre-processing included: 3D motion correction, slice scan-time correction, linear trend removal, high-pass filtering (five cycles per run), and spatial smoothing with a 6 mm full width at half maximum (FWHM) Gaussian kernel. fMRI data sets were interpolated to 3 × 3 × 3 mm voxels, registered to the high-resolution anatomical image, and normalized to standard Talairach space (Talairach and Tournoux, 1988). Voxels are reported as 1 × 1 × 1 mm. Data were analysed using the general linear model; the model was obtained by convolving the boxcar function of the time course of tactile stimulation with the standard haemodynamic response function. To identify between group differences in activation patterns a fixed effects analysis was performed with the contrasts: (i) healthy controls: stimulation > rest; (ii) PNIr: stimulation > rest; and (iii) healthy controls > PNIr. Activation maps were thresholded at a corrected value of $P < 0.05$ (derived from an uncorrected $P < 0.0001$ and 120 mm^3 contiguous voxels as previously reported: Taylor and Davis, 2009); this was also validated by running a Monte Carlo Simulation with AlphaSim application implemented in the Analysis of Functional Neuroimage (AFNI) software. This analysis included only the 11 patients that sustained transection of the right median nerve ($n = 9$) or the right median and ulnar nerve ($n = 2$) (i.e. the three patients with a pure right ulnar nerve transection were not included in this analysis).

Cortical thickness analysis

Cortical thickness analysis was performed using Freesurfer (http://surfer.nmr.mgh.harvard.edu); methods have been outlined in detail elsewhere (Dale *et al*., 1999; Fischl *et al*., 1999*a, b*; Fischl and Dale 2000). Briefly, high-resolution T_1-weighted anatomical data sets were registered to the Talairach atlas (Talairach and Tournoux, 1988). This was followed by intensity normalization, skull stripping and separation of the hemispheres. Subsequently, the white/grey matter (called the white surface) and grey/CSF (called the pial surface) boundaries were identified and segmented. The distance between the white and pial surfaces was then calculated at every point in each hemisphere of the brain. To identify group differences between the 14 patients and 14 age/sex-matched controls, a general linear model analysis was

performed at every point on the brain. As individual's cortical topography is inherently heterogeneous, a 5 mm FWHM spatial smoothing kernel was applied prior to statistical analysis. Data are displayed at a corrected $P<0.05$ (derived from an uncorrected $P<0.0075$ and 102 contiguous vertices); this was calculated by running a Monte Carlo simulation with AlphaSim. A vertex represents a point on a two dimensional sheet, and, in this study, the distance between two vertices is 0.80 mm^2.

As patients exhibited significant deficits in somatosensory function within the transected nerve territory, we hypothesized that measures of somatosensory function (vibration and touch detection) would correlate with cortical thickness in the contralesional post-central gyrus (primary and secondary somatosensory cortices). Therefore, we performed correlation analyses in the patient group between: (i) cortical thickness and vibration detection threshold; and (ii) cortical thickness and touch detection thresholds. One patient did not complete psychophysical assessment; therefore, this analysis included 13 PNIr patients. In addition, to determine if there was a relationship between cortical thickness and recovery time a correlation analysis was also performed between these two measures. These correlation analyses were restricted to the contralesional post-central gyrus by including a mask (taken from Freesurfer's built in atlas) in the general linear model. A Monte Carlo simulation was performed that was restricted to the number of vertices within contralesional post-central gyrus; images are displayed with a corrected $P<0.05$ (derived from an uncorrected $P<0.0075$ and 68 contiguous vertices).

Diffusion tensor imaging analysis

Diffusion tensor image processing was performed with DTiStudio (www.MriStudio.org) and FSLv.4.0 (www.fmrib.ox.ac.uk/fsl/). Images were first realigned with the Automatic Image Registration tool implemented in DTiStudio, using the first B0 image in the first series acquired as the template. This process corrects for subject motion and eddy-current distortion. All images were then inspected visually to assess image quality and the alignment of the separate diffusion tensor imaging runs. If an artefact was detected, the slice was removed prior to calculating the average of the two separate diffusion tensor imaging runs. Individual FA maps were calculated using the DTIFIT tool implemented in FSL. Voxel-wise statistical analysis was performed to identify group differences in the mean fractional anisotropy using Tract Based Spatial Statistics; for a full description of these methods see Smith *et al*. (2006). Briefly, images were non-linearly registered to a target image (MNI152), the mean image was then created from all datasets and this image was subsequently thinned to represent all tracts that were common to all subjects. Each subject's highest fractional anisotropy values were then projected onto the skeleton by searching in white matter perpendicular to each point on the white matter skeleton. A whole-brain voxel-wise statistical analysis was then performed between groups (14PNIr and 14 healthy controls) and images were whole brain corrected at $P<0.05$. In addition, a region of interest analysis was performed in white matter tracts adjacent to the contralateral S1, thalamus and bilateral anterior and posterior insula. These regions were chosen as they have previously been implicated in aspects of somatosensation and because they correspond with regions that were identified in the fMRI and cortical thickness analysis (CTA) group analyses. Regions of interest were drawn on the white matter skeleton as follows: (i) The contralateral S1 region of interest originated medially at the junction between the white matter skeleton of the corona-radiata and the skeleton section feeding into the post-central gyrus; terminating at the end of the tract within a given slice. In the z direction the region of interest extended from $z=49$ to 57; white matter tracts supplying the hand region. (ii) The contralateral thalamus region of interest was restricted to white matter tracks surrounding the posterior and medial thalamic nuclei (nuclei involved in somatosensory function), extending from $z=-1$ to 4. (iii) Insular regions of interest were drawn bilaterally within white matter adjacent to the anterior and posterior insula based on criteria previously published by our lab (Taylor *et al*., 2008*b*). The region of interest extended from $z=2$ to 8. Fractional anisotropy values were extracted from each of these regions of interest and a multivariate analysis of variance (MANOVA) was performed using the Statistical Package for the Social Sciences v13.0 (SPSS Inc, Chicago), which included fractional anisotropy values for all six regions of interest.

Results

Table 1 provides demographic details for study participants. All 14 patients sustained a complete transection of the right median and/or ulnar nerve followed by microsurgical repair at least 1.5 years prior to study enrolment. The time from surgery to testing ranged from 1.5 to 8 years with a mean (±SD) of 4.8 ± 3 years. Patients and controls did not differ in age (34 ± 10 years both groups; $t=0.04$; $P=0.97$).

Psychophysics

Vibration thresholds were calculated from all three measurements since one-way repeated measures analysis of variance (ANOVA) indicated no significant differences between the three trials [F (25, 1) = 0.227, $P=0.64$]. Vibration and mechanical detection thresholds were significantly impaired in PNIr patients compared to healthy controls (vibration: $t=4.77$, $P<0.001$, Fig. 3A; mechanical: $t=3.10$, $P=0.005$, Fig. 3D).

Nerve conduction testing

Amplitude and latency measures obtained from each patient's contralesional nerves were classified as normal by an experienced neurologist at the Toronto Western Hospital EMG Clinic. Nine of the 14 patients completed nerve conduction testing. Table 2 displays the average increase/decrease latency and amplitude data for sensory nerve conduction from the wrist to the abductor pollicis brevis (median) or abductor digiti minimi (ulnar) muscles and for sensory conduction from the wrist to D2 (median) and D5 (ulnar) compared to each patients uninjured contralesional nerve. Out of nine, seven patients had transections that included the median nerve. Of these seven, one patient had no detectable response during motor testing and another patient had no detectable response during sensory testing. In the six patients with detectable responses, motor conduction latencies were increased by 43% ($t=6.2$; $P=0.002$) and amplitudes were decreased by 38% ($t=-2.6$; $P=0.045$) when each patient's transected nerve was compared to their non-injured side. Sensory conduction in median nerves also revealed a 26% increase in latency ($t=3.9$; $P=0.011$) and a 73% decrease in amplitude ($t=-8.0$; $P=0.000$) compared to normal contralesional nerves. In the four patients with ulnar nerve transections one patient had no detectable

Table 2 Summary of nerve conduction data

	Sensory nerve (wrist to digit 2 or 5) PNIr	Motor nerve (wrist to APB or ADM) PNIr
Total number patients tested	9 (of 14)	9 (of 14)
Median		
Transections (*n*)	7	7
No response (*n*)	1	1
Responded (*n*)	6	6
Per cent average increase in latency	26*	43*
Per cent average decrease in amplitude	73*	38*
Ulnar		
Transections (*n*)	4	4
No response (*n*)	1	0
Responded (*n*)	3	4
Per cent average increase in latency	27*	42
Per cent average decrease in amplitude	30	41*

Percentage of increased or decreased latency and amplitude are based on a direct comparison with each patient's contralesional, untransected nerve.
*$P < 0.05$.
Statistics are based on paired *t*-tests and a two-tail distribution (see text for exact *t*-scores and *P*-values).
PNIr = peripheral nerve injury and surgical repair patients, APB = abductor pollicis brevis, ADM = abductor digiti minimi.

response during sensory nerve testing. In those patients with responses, ulnar nerve motor latencies were not significantly elevated ($t = 2.8$; $P = 0.070$); however, amplitudes were significantly decreased by 41% ($t = -5.9$; $P = 0.010$). Sensory testing of the ulnar nerve demonstrated a 27% increase in latency ($t = 4.3$; $P = 0.049$) but no significant increase in amplitude ($t = -3.5$; $P = 0.072$).

Functional plasticity in the primary somatosensory cortex

Functional MRI maps were calculated from the 11 PNIr patients with right median nerve transections (patients with ulnar nerve transections were excluded from this analysis) and 11 age- and sex-matched healthy controls. From Fig. 1A, it is clear that PNIr patients have significantly less activation, compared to healthy controls, in a region of S1 corresponding to Brodmann area 2 (BA2) (Talairach and Tournoux, 1988) and S2 (see Table 3 for details). The average event-related responses from these regions of interest highlight the attenuated BOLD response within the patients' left BA2 and left S2 (Fig. 1B and C, respectively). Curiously, vibrotactile stimulation in the patients activated a more superior part of the post-central gyrus (probably BA1/3) (Talairach and Tournoux, 1988) (Fig. 1A and Table 3). An event-related average (Fig. 1D) demonstrates that healthy controls had minimal activation in this region. Furthermore, patients had significantly more activation in brain regions collectively known as the task positive network (asterisks in Fig. 1). See Table 3 for the full list of task positive brain areas activated. This network includes lateral prefrontal, lateral parietal, premotor and inferior temporal cortices (Table 3): brain areas that are activated during the performance of an attention demanding task and suppressed or inactive during rest or tasks that are not cognitively or attentionally challenging (Fox *et al*., 2005; DeLuca *et al*., 2006; Seminowicz and Davis 2007).

Reduced grey matter in the primary somatosensory cortex correlates with sensory recovery

Cortical thickness analysis in all 14 patients and 14 age/sex-matched healthy controls revealed several loci of significant cortical thinning in the PNIr group (Fig. 2 and Table 4). Specifically, patients had a 13%–22% reduction in cortical thickness in the left (contralesional) S1, S2, pregenual anterior cingulate gyrus, ventrolateral prefrontal cortex and right anterior insula, anterior/posterior mid cingulate gyrus and paracentral lobule. Interestingly, the locations of grey matter thinning within the post-central gyrus coincide with the regions of reduced BOLD following vibrotactile stimulation (Table 4). Since we had prior knowledge of the patients' sensory deficits and recovery time (i.e. time since microsurgical repair), we next asked whether the patients' cortical thickness in the post-central gyrus correlated with their sensory mechanical and vibration detection thresholds, or with their recovery time. These analyses revealed a negative correlation between cortical thickness and vibration detection thresholds in a region encompassing BA1/2 and S2 ($P < 0.001$, $r = -0.80$ and -0.91, for BA1/2 and S2, respectively; Fig. 3 and Table 5). In addition, mechanical detection thresholds were also negatively correlated with cortical thickness in a slightly more superior BA2 region and the same S2 region ($P < 0.001$, $r = -0.83$ and -0.85, for BA2 and S2, respectively; Fig. 3 and Table 5). However, we did not identify a significant relationship between recovery time and cortical thickness. Therefore, in the post-central gyrus cortical thinning was associated with more severe sensory deficits. However, we did not identify a significant relationship between recovery time and cortical thickness. Again, there was a correspondence between the cortical thinning in areas negatively correlated with vibratory stimuli and the regions showing group fMRI and CTA abnormalities.

White matter abnormalities following nerve transection

To assess white matter integrity we utilized a region of interest approach to examine white matter group differences based on *a priori* hypotheses. Regions of interest were restricted to white matter tracts surrounding and feeding into the contralesional S1 and thalamus. In addition, we also drew regions of interest in white matter adjacent to left and right, anterior and posterior insula. The insula was chosen as it is implicated in somatosensory processing and because we identified reduced grey matter in the right anterior insular with CTA. This region of interest approach revealed that patients had significantly reduced white matter fractional anisotropy values (MANOVA including all six regions of interest) adjacent to the right anterior [F (1, 26) = 4.39,

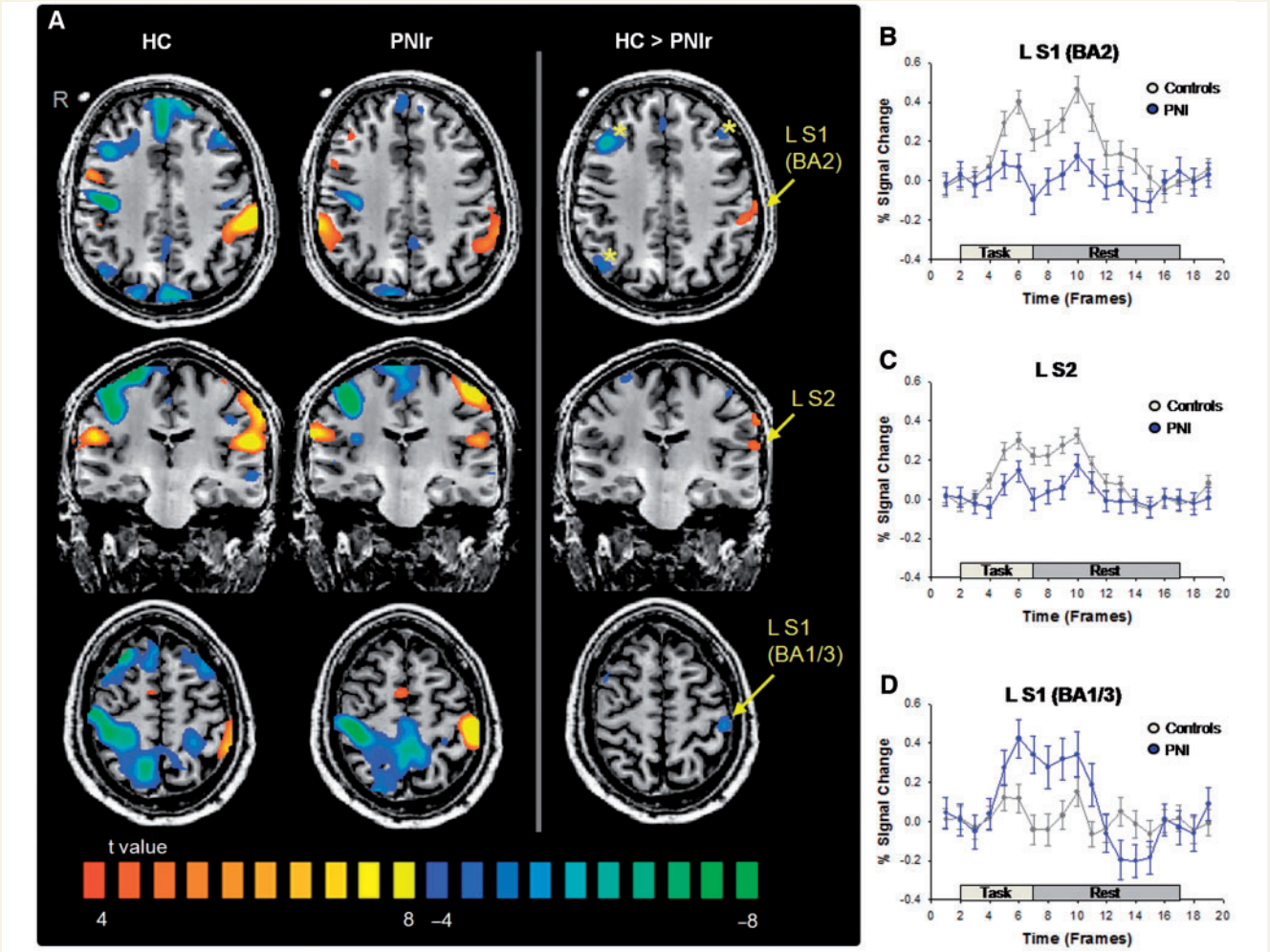

Figure 1 BOLD response to a 12 Hz pneumatic vibrotactile stimulus applied to the transected nerve territory (right D2). Fixed effects block design was used with 10 s of tactile stimuli and 20 s of rest [thresholded at a corrected $P<0.05$ (based on $P<0.0001$ and 120 mm^3 clusters)]. (**A**) The first and second columns display regions of significant activation/deactivation (compared to rest) in healthy controls (HC) and PNIr, respectively. The third column displays significant group differences with the contrast HC > PNIr. Event-related averages demonstrated that HC activate L S1 (BA 2) (**B**), and the L S2 (**C**) significantly more than PNIr patients; whereas PNIr patients activated L S1 (BA 1/3) more than HC (**C**). Asterisks denote lateral frontal and parietal brain areas included in the task positive network. For a full list of task positive brain areas demonstrating greater activation in patients than controls see Table 3.

$P=0.046$; Fig. 4A] and posterior insula [F (1, 26) = 5.55, $P=0.026$; Fig. 4B], but there were no group differences in the white matter adjacent to the left insula (left anterior insula: $P=0.51$; left posterior insula: $P=0.26$), thalamus ($P=0.46$) or S1 ($P=0.46$).

Discussion

Here, we have demonstrated for the first time that there is functional plasticity and both grey and white matter structural abnormalities in several cortical areas following upper limb peripheral nerve transection and surgical repair. This plasticity may arise from incomplete peripheral nerve regeneration (peripheral cell death and/or incomplete re-myelination), as nerve conduction measures in these patients demonstrated severe abnormalities. In addition, our data demonstrate that decreased vibrotactile-evoked fMRI responses in the post-central gyrus correspond with grey matter thinning in the patient group. These results suggest that reduced BOLD responses may be facilitated by a reduction in cortical grey matter and/or a decrease in the afferent input to the post-central gyrus. In addition, cortical thickness within these same parts of the post-central gyrus negatively correlated with behavioural measures of somatosensory function. That is, increased somatosensory deficits were correlated with thinner cortex; both of which may be related to afferent input. Taken together, our data suggest that incomplete peripheral nerve regeneration contributes to somatosensory impairments, cortical grey matter atrophy and reduced fMRI activation (see Fig. 5 for a summary of these findings).

It is well known that cortical plasticity following peripheral nerve transection and surgical repair can occur throughout the CNS in non-human primates (Kaas, 1991). This plasticity is thought to be

Table 3 Locations of responses to a 12 Hz vibrotactile stimulus (HC > PNIr patients)

Anatomical location	Brodmann area	Activation/deactivation	No. of voxels	Talairach coordinates		
				x	y	z
Left post-central gyrus	BA 2 (S1)	Activation	1145	−56	−27	35
Left post-central gyrus	BA 40 (S2)	Activation	244	−60	−19	16
Left post-central gyrus	BA 3/1 (S1)	Deactivation	812	−41	−25	56
Left middle frontal gyrus	BA 9/10/46	Deactivation	4320	−40	41	23
Left middle frontal gyrus	BA 6	Deactivation	243	−44	8.6	48
Right precentral gryus	BA 4/6	Deactivation	197	27	−20	64
Right inferior parietal	BA 39/40	Deactivation	2538	44	−61	35
Right middle frontal gyrus	BA 46/9/8/6	Deactivation	6435	40	23	37
Right medial frontal gyrus	BA 8	Deactivation	550	3.4	37	39
Right superior frontal gyrus	BA 10	Deactivation	2095	22	56	17
Right inferior temporal gyrus	BA 39	Deactivation	498	44	−51	−14
Right cerebellum		Deactivation	220	14	−52	−17

Anatomical description and centre of gravity coordinates are displayed for all areas of significant activation/deactivation (corrected $P < 0.05$).
Brain areas that are part of the task positive network are identified in bold text. These brain areas were identified based on Talairach coordinates and BAs reported in Fox *et al*. (2005); DeLuca *et al*. (2006); and Seminowicz and Davis (2007).
S1 = primary somatosensory cortex, S2 = secondary somatosensory cortex.

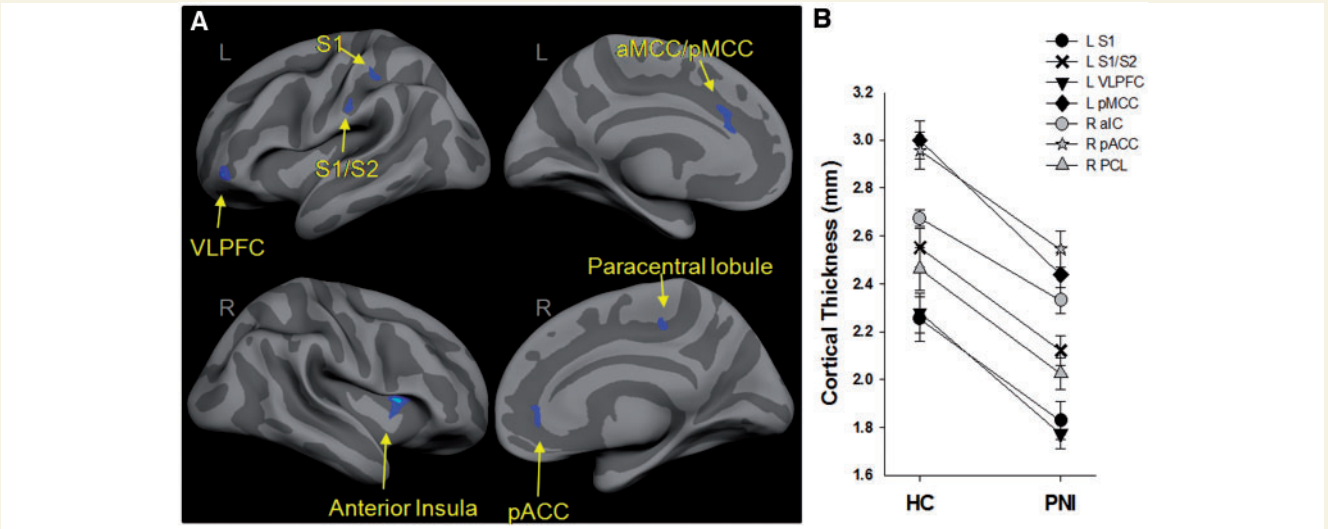

Figure 2 Cortical thickness analysis. (**A**) Cortical areas that demonstrated significant thinning in PNIr patients compared to age/sex-matched healthy controls (corrected $P < 0.05$). (**B**) The average cortical grey matter thickness (in mm), shown separately for HC and PNIr groups, is displayed for each brain region identified in (**A**). Primary (S1) and secondary (S2) somatosensory cortex, VLPFC, anterior insula (aIC), pregenual anterior cingulate cortex (pACC), anterior (aMCC) and posterior (pMCC) mid-cingulate cortex and paracentral lobule (PCL).

due to the unmasking of previously silent synapses or axonal sprouting into deafferented territory (Wall *et al*., 1986; Florence and Kaas, 1995). In the primate model, 1 year following nerve transection and surgical repair, the denervated cortex is characterized by incomplete and disorderly representations of the regenerated and adjacent (intact) nerves. This patchy representation is attributed to incomplete peripheral regeneration resulting in a partial recovery of the denervated cortical space (Kaas, 1991). To assess the extent of peripheral regeneration in our patient population we performed sensory and motor nerve conduction studies across the transected area. Our nerve conduction results demonstrate that PNIr patients have significantly decreased amplitude and increased latency in both sensory and motor nerves compared to their own untransected side. Decreased amplitude combined with increased latency is indicative of peripheral fibre loss (i.e. cell death) and/or abnormal or incomplete re-myelination following transection (Kimura, 1984). In addition, it is well established that between 20% and 50% of dorsal root ganglion neurons die following nerve transection (Liss *et al*., 1996). Thus, afferent cell death and incomplete regeneration can result in decreased afferent input to the cortex, which may account for ongoing sensory deficits and decreased BOLD response in BA2

Table 4 Cortical thickness analysis (14 HC > 14 PNIr patients)

Anatomical location	Brodmann area	Thickness (mm)		PNIr% thinning	No. of vertices	Talairach coordinates		
		HC	PNIr			x	y	z
Left post-central gyrus	BA 2/40 (S1)	2.55	2.12	17	112	−34	−32	43
Left post-central gyrus	BA 2 (S1/S2)	2.25	1.83	19	157	−54	−19	29
Left orbitofrontal gyrus	BA 10/47	2.28	1.77	22	192	−37	47	−5
Left aMCC/pMCC	BA 32	3.00	2.44	19	114	10	38	−1
Right anterior insula		2.67	2.33	13	360	30	15	7
Right pACC	BA 32	2.96	2.54	14	221	−10	25	24
Right paracentral lobule		2.46	2.02	18	111	12	−25	46

Anatomical description, location of centre of gravity coordinates, percent thinning (patients normalized to HC), and the number of vertices (where a vertex = 0.80 mm^2). HC = healthy controls, PNIr = peripheral nerve transection and surgical repair patients, pACC = pregenual anterior cingulate cortex, aMCC = anterior middle cingulate cortex, pMCC = posterior middle cingulate cortex, S1 = primary somatosensory cortex, S2 = secondary somatosensory cortex.

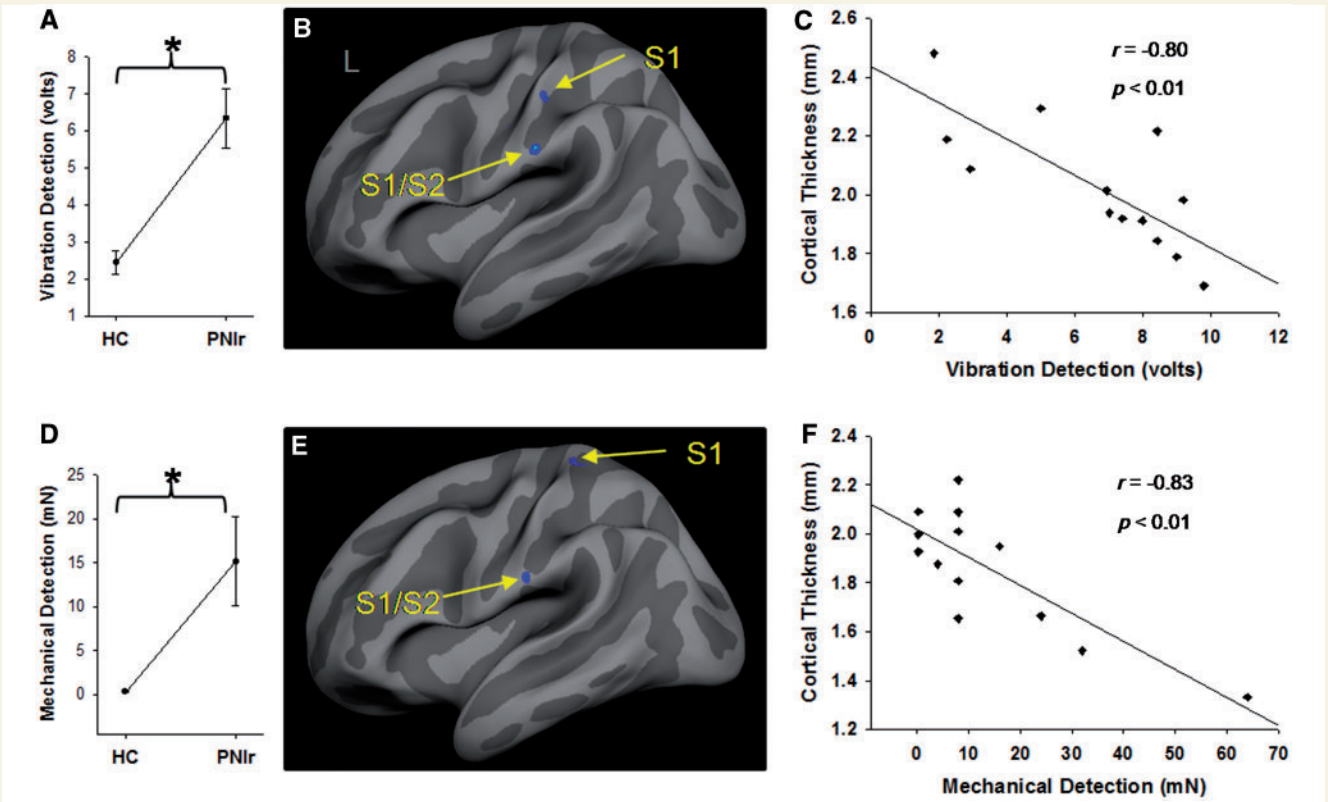

Figure 3 Cortical thickness correlated with psychophysical measures of sensory function. (**A**) and (**D**) display the average vibration and mechanical (von Frey) detection thresholds in healthy control (HC) and PNIr groups, respectively. (**B**) and (**E**) display regions within the post-central gyrus that were negatively correlated with vibration and mechanical detection, respectively (corrected $P < 0.05$). (**C**) and (**F**) demonstrate that PNIr patients' cortical thickness is negatively correlated with their vibration and mechanical detection thresholds (taken from blobs labelled S1), respectively. Asterisk indicates a $P < 0.01$.

and S2. Furthermore, this diminished afferent input could also account for the cortical thinning we observed in the same regions of the cortex. Sensory deprivation has been shown to cause transneuronal degeneration in several regions of the CNS, including the dorsal horn following sciatic nerve section (Knyihar-Csillik *et al*., 1989), and may involve second- and third-order neurons (Powell and Erulkar, 1962). Transneuronal degeneration is characterized by cell shrinkage and is thought to be related to decreased, or non-existent, afferent input (Knyihar-Csillik *et al*., 1989). Thus, cortical grey matter loss (or atrophy) could also be directly related to decreased afferent input.

We also demonstrated increased activation in the post-central gyrus in a region corresponding to BA1/3 (Talairach and Tournoux, 1988). Electrophysiological, anatomical tracing and

Table 5 Cortical thickness correlated with vibration and mechanical detection thresholds

Psychophysical assessment	Brodmann area (Functional Area)	No. of vertices	Talairach coordinates			Correlation analysis	
			x	*y*	*z*	*r*-value	*p*-value
Vibration detection	BA 1/2 (S1)	157	−21	−31	64	−0.80	0.001
Vibration detection	BA 2/40 (S1/S2)	98	−60	−19	26	−0.91	0.000
Mechanical detection	BA 2 (S1)	99	−46	−22	46	−0.83	0.000
Mechanical detection	BA 2/40 (S1/S2)	110	−57	−22	26	−0.85	0.000

Correlation analysis was restricted to the contralesional (left) post-central gyrus.

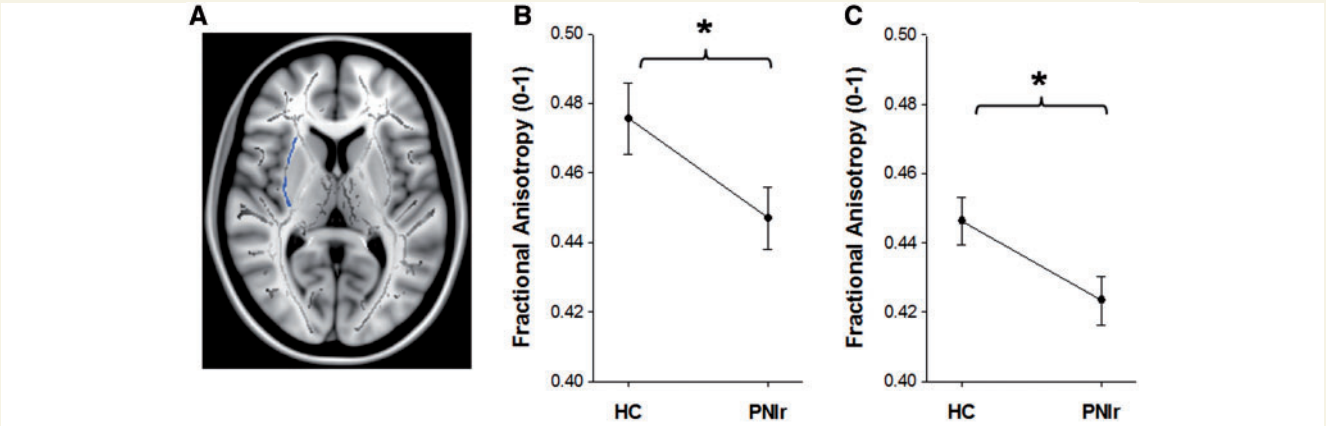

Figure 4 Diffusion tensor imaging. A region-of-interest-based approach revealed reduced fractional anisotropy in white matter adjacent to the right anterior (**B**) and posterior (**C**) insula in patients with PNIr; panel (**A**) displays the right anterior and posterior regions of interest from which the mean fractional anisotropy values were extracted. Of note also is that regions of interest in the left (contralesional) S1, thalamus and insula (anterior and posterior) did not show group differences (data not shown). $*P < 0.05$. HC = healthy controls.

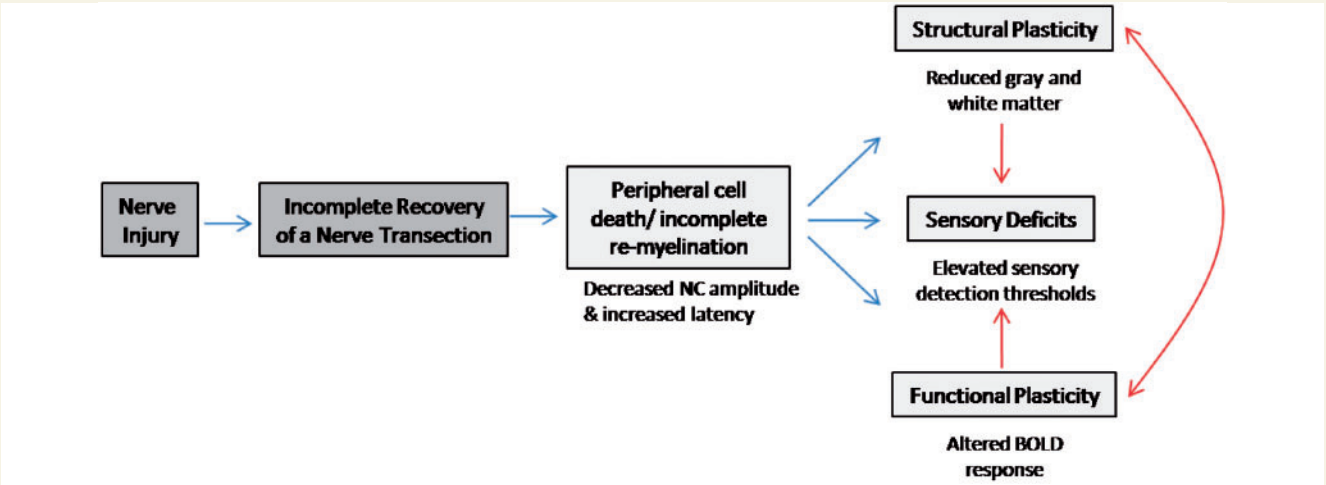

Figure 5 Summary of findings and possible causes. Nerve conduction measures remain abnormal 1.5 years following peripheral nerve transection and microsurgical repair, indicative of cell death and/or incomplete re-myelination. Incomplete peripheral nerve regneration may cause: (i) long-term sensory abnormalities; (ii) grey matter and white matter atrophy in key somatosensory regions; (iii) functional changes in key somatosensory regions. In addition, structural and functional changes may impact sensory recovery. Finally, functional and structural changes may influence each other.

neuroimaging studies have established that for the majority of cutaneous mechanoreceptive afferents the first cortical destinations are BA1 and BA3b. These cytoarchitectonic brain areas each possess a somatotopic body map with small receptive fields. In addition, these areas respond to many features of tactile information, such as texture and roughness, velocity and curvature of stimuli (Bodegard *et al*., 2001). fMRI studies have demonstrated that activity within the somatosensory cortex is influenced by attention such that fMRI responses to tactile stimuli in S1 are increased when subjects attend to a tactile stimulus, but are attenuated when subjects are distracted (Arthurs *et al*., 2004; Porro *et al*., 2004). Furthermore, our patients activated a network of brain areas known as the task positive network (DeLuca *et al*., 2006) more than healthy controls. These brain areas are activated during attention demanding processes (Fox *et al*., 2005; Seminowicz and Davis, 2007). Together, these findings imply that patients must attend to the stimulus more than controls because of their impaired sensory input. This increased attention may also account for the increased activation in BA1/3b. Of course, the increased activation in BA1/3b may also reflect plasticity that is unrelated to attentional load.

BA2 and S2 both receive projections from BA1/3b and also from distinct parts of the ventroposterior thalamic complex (Pons *et al*., 1985; Friedman and Murray, 1986). Both of these brain areas have large, often multi-digit (BA2) or bilateral (S2) receptive fields (Pons *et al*., 1985; Iwamura *et al*., 2002). Based on anatomical projections and neuronal response properties, hierarchical processing of tactile information has been demonstrated from BA1/3b to BA 2 (Kaas *et al*., 2002). In addition, electrophysiological studies in macaques (Pons *et al*., 1987) and magnetoencephalography data acquired in humans, suggest that serial processing of tactile inputs occurs from S1 to S2 in higher primates (Frot and Mauguiere 1999; Disbrow *et al*., 2001). Several studies have demonstrated that BA2 is preferentially activated by shape and curvature (Bodegard *et al*., 2001), while S2 may be involved in tactile learning (Ridley and Ettlinger 1976; Murray and Mishkin, 1984), supporting the notion that these brain areas are involved in higher-order somatosensory processing. Our psychophysical assessment demonstrated that patients were significantly impaired at the detection of simple tactile stimuli, and in the Shape Texture Identification test 1.5 years after surgery (Taylor *et al*., 2008*a*). This latter test assesses a patient's ability to recognize characteristics of an object while actively exploring a shape or texture, requiring the integration of sensory information across regions of the body (Rosen and Lundborg, 1998). Taken together, one interpretation of our data is that PNIr patients attend more to the vibrotactile stimulus, leading to increased activation of the task positive network and BA1/3. However, in these patients, our data imply that higher-order processing areas, such as BA2 and S2, did not receive tactile information, which, in turn, may result in cortical thinning and reduced BOLD responses.

The insula is thought to play a role in integrating multimodal information important for sensorimotor, emotional, allostatic/homeostatic and cognitive functions (Devinsky *et al*., 1995; Critchley, 2004; Craig, 2008) and has been designated a limbic sensory cortex (Craig, 2008). Several studies have reported insular activation in response to tactile stimulation (Gelnar *et al*., 1998; Downar *et al*., 2002) and anatomical tracing studies in primates have demonstrated that the insula is reciprocally connected to frontal, parietal and temporal lobes (Augustine, 1996). In our patients, the right anterior insula was the only cortical area that demonstrated significant cortical thinning in conjunction with reduced fractional anisotropy values in the adjacent white matter, suggesting that the cortical thinning within this region is associated with a loss of fibres projecting to or from this structure. The right anterior insula has been implicated in interoception as it is situated to integrate homeostatic input from the body with motivational, emotional and social conditions (Craig, 2008). Furthermore, Critchley *et al*. (2004) reported a correlation between interoceptive abilities and the grey matter volume of the right anterior insula. Given our finding that the patients have decreased grey matter in the right anterior insula, it would be of interest to assess interoceptive capabilities following peripheral nerve injury in a future study.

Taken together, we have demonstrated for the first time that functional and structural alterations are present in the human cerebral cortex 1.5 years after a complete transection of an upper limb peripheral nerve that was microsurgically repaired. In addition, nerve conduction measures indicate incomplete peripheral regeneration in these patients. Furthermore, we show that cortical thickness is related to psychophysical measures of recovery, in that thinner cortex within BA2 and S2 was associated with poorer somatosensory function. These data suggest that the reestablishment of normal functional activation maps is directly associated with the successful regeneration of peripheral afferents.

Acknowledgements

The authors thank Mr. Geoff Pope, Dr. Adrian Crawley, Mr. Eugene Hlasny and Mr. Keith Ta for expert technical assistance. The authors would like to thank Dr. Peter Ashby and Mr. Freddy Paiz from the Toronto Western Hospital EMG Clinic for conducting the nerve conduction tests and for providing expert assessment of the findings. The authors also thank Drs Dvali, Binhammer, Fialkov and Antonyshyn for collaborating with this project. Dr. Davis is a Canada Research Chair in Brain and Behaviour (CIHR MOP 53304).

Funding

The Physicians' Services Incorporated and a joint seed grant from the University of Toronto Centre for the Study of Pain/AstraZeneca.

Supplementary material

Supplementary material is available at *Brain* online.

References

Apkarian AV, Sosa Y, Sonty S, et al. Chronic back pain is associated with decreased prefrontal and thalamic gray matter density. J Neurosci 2004; 24: 10410–5.

Arthurs OJ, Johansen-Berg H, Matthews PM, Boniface SJ. Attention differentially modulates the coupling of fMRI BOLD and evoked potential signal amplitudes in the human somatosensory cortex 7. Exp Brain Res 2004; 157: 269–74.

Augustine JR. Circuitry and functional aspects of the insular lobe in primates including humans. Brain Res Brain Res Rev 1996; 22: 229–44.

Beaulieu C. The basis of anisotropic water diffusion in the nervous system - a technical review. NMR Biomed 2002; 15: 435–55.

Bodegard A, Geyer S, Grefkes C, Zilles K, Roland PE. Hierarchical processing of tactile shape in the human brain. Neuron 2001; 31: 317–28.

Craig AD. Interoception and Emotion: A Neuroanatomical Perspective. In: Lewis M, Haviland-Jones J, Barrett L, editors. Handbook of emotions. New York: Guildford Press; 2008. p. 272–87.

Critchley HD. The human cortex responds to an interoceptive challenge. Proc Natl Acad Sci USA 2004; 101: 6333–4.

Critchley HD, Wiens S, Rotshtein P, Ohman A, Dolan RJ. Neural systems supporting interoceptive awareness. Nat Neurosci 2004; 7: 189–95.

Dale AM, Fischl B, Sereno MI. Cortical surface-based analysis. I. Segmentation and surface reconstruction. Neuroimage 1999; 9: 179–94.

Davis KD, Pope G, Chen J, Kwan CL, Crawley AP, Diamant NE. Cortical thinning in IBS: implications for homeostatic, attention, and pain processing. Neurology 2008; 70: 153–4.

DeLuca M, Beckmann CF, De SN, Matthews PM, Smith SM. fMRI resting state networks define distinct modes of long-distance interactions in the human brain. Neuroimage 2006; 29: 1359–67.

Devinsky O, Morrell MJ, Vogt BA. Contributions of anterior cingulate cortex to behaviour. Brain 1995; 118 (Pt 1): 279–306.

Disbrow E, Roberts T, Poeppel D, Krubitzer L. Evidence for interhemispheric processing of inputs from the hands in human S2 and PV. J Neurophysiol 2001; 85: 2236–44.

Downar J, Crawley AP, Mikulis DJ, Davis KD. A cortical network sensitive to stimulus salience in a neutral behavioral context across multiple sensory modalities. J Neurophysiology 2002; 87: 615–20.

Draganski B, Moser T, Lummel N, et al. Decrease of thalamic gray matter following limb amputation. Neuroimage 2006; 31: 951–7.

Fischl B, Dale AM. Measuring the thickness of the human cerebral cortex from magnetic resonance images. Proc Natl Acad Sci USA 2000; 97: 11050–5.

Fischl B, Sereno MI, Dale AM. Cortical surface-based analysis. II: Inflation, flattening, and a surface-based coordinate system. Neuroimage 1999a; 9: 195–207.

Fischl B, Sereno MI, Tootell RB, Dale AM. High-resolution intersubject averaging and a coordinate system for the cortical surface. Hum Brain Mapp 1999b; 8: 272–84.

Florence SL, Kaas JH. Large-scale reorganization at multiple levels of the somatosensory pathway follows therapeutic amputation of the hand in monkeys. J Neurosci 1995; 15: 8083–95.

Fox MD, Snyder AZ, Vincent JL, Corbetta M, Van E, Raichle ME. The human brain is intrinsically organized into dynamic, anticorrelated functional networks. Proc Natl Acad Sci USA 2005; 102: 9673–9678.

Friedman DP, Murray EA. Thalamic connectivity of the second somatosensory area and neighboring somatosensory fields of the lateral sulcus of the macaque. J Comp Neurol 1986; 252: 348–73.

Frot M, Mauguiere F. Timing and spatial distribution of somatosensory responses recorded in the upper bank of the sylvian fissure (SII area) in humans. Cereb Cortex 1999; 9: 854–63.

Geha PY, Baliki MN, Harden RN, Bauer WR, Parrish TB, Apkarian AV. The brain in chronic CRPS pain: abnormal gray-white matter interactions in emotional and autonomic regions. Neuron 2008; 60: 570–81.

Gelnar PA, Krauss BR, Szeverenyi NM, Apkarian AV. Fingertip representation in the human somatosensory cortex: an fMRI study. Neuroimage 1998; 7: 261–83.

Hickmott PW, Steen PA. Large-scale changes in dendritic structure during reorganization of adult somatosensory cortex. Nat Neurosci 2005; 8: 140–42.

Iwamura Y, Tanaka M, Iriki A, Taoka M, Toda T. Processing of tactile and kinesthetic signals from bilateral sides of the body in the postcentral gyrus of awake monkeys. Behav Brain Res 2002; 135: 185–90.

Jaquet JB, Luijsterburg AJ, Kalmijn S, Kuypers PD, Hofman A, Hovius SE. Median, ulnar, and combined median-ulnar nerve injuries: functional outcome and return to productivity. J Trauma 2001; 51: 687–92.

Jurkiewicz MT, Crawley AP, Verrier MC, Fehlings MG, Mikulis DJ. Somatosensory cortical atrophy after spinal cord injury: a voxel-based morphometry study. Neurology 2006; 66: 762–4.

Kaas JH. Plasticity of sensory and motor maps in adult mammals. Annu Rev Neurosci 1991; 14: 137–67.

Kaas JH, Jain N, Qi HX. The organization of the somatosensory system in primates. In: Nelson RJ, editor. The somatosensory system. Washington, D.C.: CRC Press; 2002. p. 1–25.

Kimura J. Electrodiagnosis in diseases of the nerve and muscle: principles and practice. Oxford: Oxford University Press; 2001.

Kimura J. Principles and pitfalls of nerve conduction studies. Ann Neurol 1984; 16: 415–29.

Knyihar-Csillik E, Rakic P, Csillik B. Transneuronal degeneration in the Rolando substance of the primate spinal cord evoked by axotomy-induced transganglionic degenerative atrophy of central primary sensory terminals. Cell Tissue Res 1989; 258: 515–25.

Liss AG, af Ekenstam FW, Wiberg M. Loss of neurons in the dorsal root ganglia after transection of a peripheral sensory nerve. An anatomical study in monkeys. Scand J Plast Reconstr Surg Hand Surg 1996; 30: 1–6.

Lotze M, Flor H, Grodd W, Larbig W, Birbaumer N. Phantom movements and pain. An fMRI study in upper limb amputees. Brain 2001; 124: 2268–77.

Manduch M, Bezuhly M, Anastakis DJ, Crawley AP, Mikulis DJ. Serial fMRI of adaptive changes in primary sensorimotor cortex following thumb reconstruction. Neurology 2002; 59: 1278–81.

May A. Chronic pain may change the structure of the brain. Pain 2008; 137: 7–15.

McAllister RM, Gilbert SE, Calder JS, Smith PJ. The epidemiology and management of upper limb peripheral nerve injuries in modern practice. J Hand Surg (Br) 1996; 21: 4–13.

Murray EA, Mishkin M. Relative contributions of SII and area5 to tactile discrimination in monkeys 2. Behav Brain Res 1984; 11: 67–83.

Napadow V, Kettner N, Ryan A, Kwong KK, Audette J, Hui KK. Somatosensory cortical plasticity in carpal tunnel syndrome-a cross-sectional fMRI evaluation. Neuroimage 2006; 31: 520–30.

Oldfield RC. The assessment and analysis of handedness: the Edinburgh inventory. Neuropsychologia 1971; 9: 97–113.

Pons TP, Garraghty PE, Cusick CG, Kaas JH. The somatotopic organization of area 2 in macaque monkeys 6. J Comp Neurol 1985; 241: 445–66.

Pons TP, Garraghty PE, Friedman DP, Mishkin M. Physiological evidence for serial processing in somatosensory cortex. Science 1987; 237: 417–20.

Porro CA, Lui F, Facchin P, Maieron M, Baraldi P. Percept-related activity in the human somatosensory system: functional magnetic resonance imaging studies. Magn Reson Imaging 2004; 22: 1539–48.

Powell TP, Erulkar S. Transneuronal cell degeneration in the auditory relay nuclei of the cat. J Anat 1962; 96: 249–68.

Ridley RM, Ettlinger G. Impaired tactile learning and retention after removals of the second somatic sensory projection cortex (SII) in the monkey. Brain Res 1976; 109: 656–60.

Rosen B, Lundborg G. A new tactile gnosis instrument in sensibility testing. J Hand Ther 1998; 11: 251–7.

Seminowicz DA, Davis KD. Pain enhances functional connectivity of a brain network evoked by performance of a cognitive task. J Neurophysiol 2007; 97: 3651–9.

Smith SM, Jenkinson M, Johansen-Berg H, et al. Tract-based spatial statistics: voxelwise analysis of multi-subject diffusion data. Neuroimage 2006; 31: 1487–1505.

Talairach J, Tournoux P. Co-planar stereotaxic atlas of the human brain. New York: Thieme Medical Publishers Inc.; 1988.

Taylor KS, Anastakis DJ, Davis KD. Chronic pain following peripheral nerve injury is associated with pain catastrophizing and neuroticism. Int Ass Stud Pain 2008a; 267.

Taylor KS, Davis KD. Stability of tactile- and pain-related fMRI brain activations: an examination of threshold-dependent and threshold-independent methods. Hum Brain Mapp 2009; 30: 1947–62.

Taylor KS, Seminowicz DA, Davis KD. Two systems of resting state connectivity between the insula and cingulate cortex. Hum Brain Mapp 2008b;DOI:10.1002/hbm.20705.

Wall JT, Kaas JH, Sur M, Nelson RJ, Felleman DJ, Merzenich MM. Functional reorganization in somatosensory cortical areas 3b and 1 of adult monkeys after median nerve repair: possible relationship to sensory recovery in humans. J Neurosci 1986; 6: 218–33.